
What is a Goldilocks Face Verification Test Set?

Haiyu Wu¹ Sicong Tian² Aman Bhatta¹ Jacob Gutierrez¹ Grace Bezold¹
Genesis Argueta¹ Karl Ricanek Jr.³ Michael C. King⁴ Kevin W. Bowyer¹

¹University of Notre Dame

²Indiana University South Bend

³University of North Carolina Wilmington

⁴Florida Institute of Technology

Abstract

Face Recognition models are commonly trained with web-scraped datasets containing millions of images and evaluated on test sets emphasizing pose, age and mixed attributes. With train and test sets both assembled from web-scraped images, it is critical to ensure disjoint sets of identities between train and test sets. However, existing train and test sets have not considered this. Moreover, as accuracy levels become saturated, such as LFW > 99.8%, more challenging test sets are needed. We show that current train and test sets are generally not identity- or even image-disjoint, and that this results in an optimistic bias in the estimated accuracy. In addition, we show that identity-disjoint folds are important in the 10-fold cross-validation estimate of test accuracy. To better support continued advances in face recognition, we introduce two “Goldilocks¹” test sets, Hadrian and Eclipse. The former emphasizes challenging facial hairstyles and latter emphasizes challenging over- and under-exposure conditions. Images in both datasets are from a large, controlled-acquisition (not web-scraped) dataset, so they are identity- and image-disjoint with all popular training sets. Accuracy for these new test sets generally falls below that observed on LFW, CPLFW, CALFW, CFP-FP and AgeDB-30, showing that these datasets represent important dimensions for improvement of face recognition. The datasets are available at: <https://github.com/HaiyuWu/SOTA-Face-Recognition-Train-and-Test>

1 Introduction

Face recognition (FR) training sets are web-scraped with millions of images [6, 7, 2, 49]. It is inevitable to have some same identities or images as existing datasets when collecting in-the-wild images for new datasets. However, none of datasets considers/reports this condition. Hence, it is needed to investigate whether data overlap exists between train and test sets, and how it affects the estimated accuracy. To do so, we first use a FR model to extract the features of the images in the popular training sets (i.e., MS1MV2 [6], Glint360K [2], WebFace4M [49]) and test sets (i.e., LFW [12], CFP-FP [33], AgeDB-30[25]). Then, we compare all the training images against the test images and select the two most similar training images for each test image. To get an accurate overlap estimation, human annotators evaluate all the selected image pairs. Those pairs marked as identity overlap between train and test are used to conduct an experiment on the effect of on the estimated FR accuracy. We consistently observe lower accuracy when train and test sets are identity disjoint. Moreover, the effect is larger when the training set is cleaner and when the test set is more challenging.

¹https://en.wikipedia.org/wiki/Goldilocks_and_the_Three_Bears

After understanding the effect of data overlap between training and test in FR, we introduce two new Goldilocks-level (neither too easy nor too hard) test sets. These test sets emphasize important factors not emphasized in existing test, but that are known to substantially impact recognition accuracy [40, 41, 44, 35, 3, 26, 1]. The first dataset focuses on challenging conditions of facial hairstyles (Hadrian²) and the second focuses on face exposure level (Eclipse³). Contributions of this paper include:

- Demonstrating that face recognition methods gain “optimistic bias” from identity overlap between train and test sets. Notably, after removing the overlapped identities from the training set, the average accuracy decreases for all four methods evaluated.
- Introducing two new, more challenging test sets - Hadrian and Eclipse - focused on conditions not emphasized in existing face verification test sets. Images are of higher quality than typical in-the-wild images, but accuracy is lower than for LFW, CALFW, CPLFW, CFP-FP and AgeDB-30.
- Demonstrating the importance of identity-disjoint folds in computing 10-fold cross-validation accuracy for a test set. Failure to ensure identity-disjoint folds causes optimistic bias in the estimated accuracy. Therefore we define identity-disjoint folds for our new test sets.

2 Literature Review

Face Recognition Test Sets: The well-known LFW [12] was the first web-scraped dataset with a defined performance measurement protocol. With the advance of deep learning architectures for face recognition, recent face matchers achieve over 99.80% accuracy on LFW, meaning only 12 image pairs are misclassified. Consequently, additional test sets have been introduced to challenge face recognition methods on various dimensions. AgeDB [25] and CALFW [46] target age differences, where AgeDB with image pairs featuring a 30-year gap is referred to as AgeDB-30. CFP-FP [33] and CPLFW [45] emphasize pose differences. MeGlass [9] emphasizes differences caused by wearing glasses. Datasets [36, 29, 27] include look-alike image pairs from Doppelgänger or twins. MLFW [37] was generated based on LFW for face verification with masks during the COVID-19 pandemic. IJB-S [15], XQLFW [20], TinyFace [5], and SCFace [8] compile challenges for low-quality face recognition. Near-infrared face pair verification presents another challenge. Benchmark datasets [21, 11, 4]. BA-test [39], BFW [31], and DemogPairs [14] test the face recognition model’s accuracy across different demographics. To our knowledge there is no existing dataset that emphasizes challenging facial hairstyles or under-/over-exposure conditions.

Image and Identity Duplicates: Recent analysis of face recognition datasets [32] explores the impact of duplicate and near-duplicate images. The study found that removing duplicate images within training identities has a relatively minor effect on the estimated accuracy of the trained model. The existence of duplicate and near-duplicate images in the CelebA [22] dataset was previously analyzed [42]. No prior work has focuses on examining the overlap of identities and images between commonly-used face recognition training and test sets.

This paper identifies the image and identity overlap between training and testing sets and investigates the impact of these overlapped identities on performance measurement. Additionally, two new test sets are introduced, focusing on challenging facial hairstyle conditions and face exposure differences, with more stringent pair selection rules to provide more rigorous face verification datasets.

3 Optimistic Bias from Identity Overlap

In object recognition tasks, train and test sets should be image disjoint (no image overlap) in order to obtain an unbiased estimate of model accuracy. Since face recognition models are used to recognize people not in the training set, identity disjoint train and test should be considered. However, to the best of our knowledge, existing datasets do not address the issue of identity-disjoint train and test. Therefore, this section explores whether identity overlap exists for current widely-used train and test

²Hadrian was the first Roman emperor to be depicted with facial hair.

³An eclipse epitomizes the stark contrast between intense illumination and profound darkness.

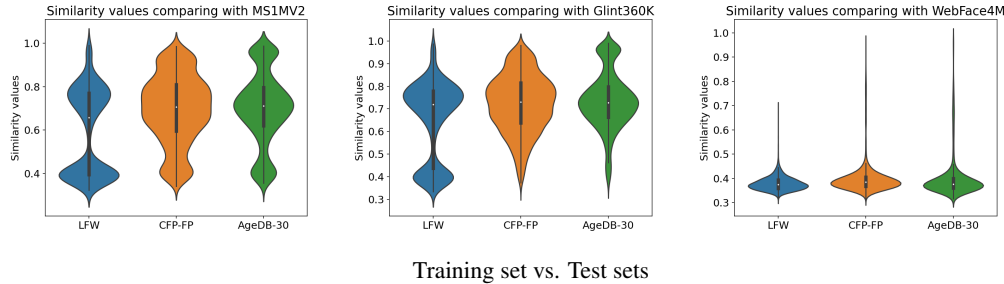


Figure 1: Identity and Image Overlap Between Train and Test Sets. Left to right, violin plots for training sets MS1MV2, Glint-360k and WebFace4M. The violin plots show distribution of similarity scores for images in test sets LFW, CFP-FP, and AgeDB-30 for each training set (two highest similarity scores for each test image matched against each training set). The portion of a distribution above 0.9 indicates likely duplicate or near-duplicate images between test and train. The portion of a distribution between 0.7 and 0.9 indicates likely identity overlap between test and train. Identity overlap exists between all train and test sets considered; image overlap exists for all but LFW and WebFace4M.

sets and how it affects estimated accuracy. Examples of detected identities and images are in the Supplementary Material.

3.1 Identity Overlap Detection

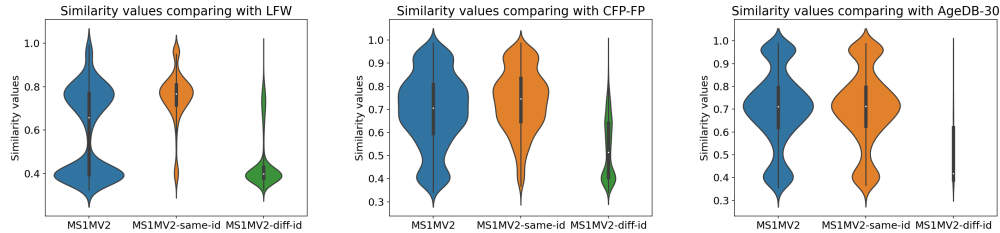
Commonly used train and test sets include MS1MV2 [6], Glint360K [2] and WebFace4M [49] for training, and LFW [12], CFP-FP [33], AgeDB-30 [25], CPLFW [45], and CALFW [46] for test. Since CPLFW and CALFW share the same identities as LFW, only LFW, CFP-FP, and AgeDB-30 are considered in this experiment to determine train/test identity overlap. The vast number of images in the training sets makes it impractical to manually check all image pairs. To simplify the process, we employ ArcFace-R100 trained with Glint360K⁴ to select, for each image in a test set, the two highest similarity images from each training set. Figure 1 shows that MS1MV2 and Glint360K contain significant fractions of the test **identities** and **images**, but that overlap is lower for WebFace4M. We speculate that WebFace260M, being a new web-scraped dataset with 4M identities, reduces the likelihood of having the same test identities and images in a cleaned subset, WebFace4M.

To verify the accuracy of the face matching results and explore an automated method to address the identity overlap issue, human annotators evaluated the selected image pairs from three test sets and the MS1MV2 training set. Each image pair was classified as same identity or different identities, and pairs identified as same identity also marked as same image or not. The manual labels indicate that 5% (384) of LFW images and 47% (2,009) of LFW identities overlap with MS1MV2, 33.42% (1,459) of CFP-FP images and 99.8% (499) of CFP-FP identities overlap with MS1MV2, and 18.88% (1,000) of AgeDB-30 images and **all** (388) AgeDB-30 identities overlap with MS1MV2. Figure 2 presents the similarity distributions of the selected pairs, highlighting that same-identity pairs exhibit higher similarity values than different-identity pairs, although there is an overlap in the range of 0.5 to 0.8. It is still feasible to exclude a large fraction of overlapping identities using a threshold value of 0.5. Consequently, a threshold of 0.5 is a reasonable criterion to automatically exclude a significant portion of overlapping identities from the dataset. From Figure 1, WebFace4M would have lower identity overlap with current test sets, and is a good choice of training set from this perspective.

3.2 Effect on Accuracy

The preceding section shows that both identity and image overlaps exist between commonly-used train and test sets. The question is: how significantly does this overlap impact accuracy estimates? To answer this, we created three specific versions of MS1MV2: 1) ID-Disjoint, with detected overlapping identities removed; 2) ID-Overlap-Raw (ID-Overlap-R), which involves dropping an equivalent number of randomly selected identities; and 3) ID-Overlap-Cleaned (ID-Overlap-C), similar to ID-Overlap-R but with reduced identity noise in the overlapped identities. We created

⁴https://github.com/deepinsight/insightface/tree/master/model_zoo



Manual Marking Results on MS1MV2

Figure 2: Manual Marking of Same / Different Person for MS1MV2 Distribution from Fig. 1. Violin plots for overlap between MS1MV2 and LFW (left), CFP-FP (center) and AgeDB-30 (right). Within each violin plot, the distribution on the left is split into similarity scores for image pairs manually marked as same person (middle) and manually marked as different persons (right). Results suggest that a threshold of 0.5 could broadly but not perfectly determine identity overlap between train and test.

three versions of MS1MV2 in this way for each of LFW, CFP-FP, and CPLFW. It was observed that identities in a test set often matched with more than one MS1MV2 identity. For instance, 2,009 LFW identities produced high-similarity matches to 2,195 MS1MV2 identities, 499 CFP-FP individuals matched 891 MS1MV2 identities, and 388 AgeDB-30 identities matched with 1,317 MS1MV2 identities. There are two causes for this. One, an identity folder in the training set sometimes contains one or more “noise” images of a different identity, and an image from the test set may match to the noise image. Two, a celebrity may be in the training set with more than one identity folder, perhaps as different characters they have played, and an image from the test set may match to their various folders. Consequently, we undertook a noise reduction step for ID-Overlap-R, utilizing DBSCAN [28] to filter the noise within an identity folder, retaining only the majority group. For LFW, 15,644 images were eliminated from the training set, altering the matching outcomes to 1,953 LFW identities matching 2,096 MS1MV2 identities. In the case of CFP-FP, 33,043 images were removed, resulting in 494 CFP-FP identities matching to 794 MS1MV2 identities. For AgeDB-30, 81,770 images were excluded from training, resulting in 384 AgeDB-30 identities matching to 1,160 MS1MV2 identities. If multiple MS1MV2 identities matched a single test identity, they were merged into one identity prior to training a network.

To ascertain the impact, we employed two constant margin methods, ArcFace and UniFace, and two adaptive margin methods, MagFace and AdaFace, to train the face recognition model with the three MS1MV2 variations. Notable minor implementation differences were found among the original code packages beyond the algorithm itself. To make a consistent fair comparison, these four methods were trained using the same training and testing configurations. The backbone used was a variant of ResNet100 [10] employed in ArcFace, with images in RGB channel and the random horizontal flip for data augmentation. For testing, squared Euclidean distance was utilized, and the feature was the summation of features from the original and horizontally flipped images. Partial-FC [2] was implemented to expedite the training process, with the remainder of the hyper-parameters aligned with the original source code.

Table 1 shows the accuracy values of the four face recognition methods, trained across nine versions of the MS1MV2 dataset, on five standard test sets. A general observation is that removing overlapped identities from the training set reduces average accuracy for all methods, with this reduction becoming larger in cleaner datasets. The discrepancy between ID-Overlap-R and ID-Disjoint suggests that, even if the overlapped identities contain noisy images or are grouped incorrectly to some degree, their presence still introduces an optimistic bias in the estimated accuracy. When the overlapped identities are further cleaned in the train set, the effect is amplified with respect to the overlapped ratio in the test sets. 45.6% LFW identities are in the MS1MV2 and the average differences between ID-Overlap-C and ID-Disjoint on LFW, CPLFW, CALFW are {0.03%, 0.13%, 0.04%}. 98.8% CFP-FP identities are in the MS1MV2 and the difference is 0.12%. 99% AgeDB-30 identities are in the MS1MV2 and the difference is 0.06%. Except CPLFW, CFP-FP and AgeDB-30 have larger differences than LFW and CALFW. Our speculation is that CPLFW gives an inconsistent result due to the difficulty of the dataset, which causes lower accuracy in general. Furthermore, Table 2 indicates that, after reducing the identity label noise, the refined portion further amplifies this optimistic bias, on par with the

Methods	Type	LFW	CFP-FP	CPLFW	AgeDB-30	CALFW	AVG
ArcFace	ID-Disjoint	99.78	98.19	93.12	98.17	96.13	97.08
ArcFace	ID-Overlap-R	99.78	98.33	93.15	98.22	96.18	97.13
ArcFace	ID-Overlap-C	99.82	98.37	93.17	98.27	96.17	97.16
UniFace	ID-Disjoint	99.80	98.44	92.80	98.17	96.00	97.04
UniFace	ID-Overlap-R	99.80	98.47	92.88	98.33	95.92	97.08
UniFace	ID-Overlap-C	99.80	98.51	93.17	98.18	95.92	97.12
MagFace	ID-Disjoint	99.78	98.26	92.87	98.20	96.03	97.03
MagFace	ID-Overlap-R	99.82	98.34	92.82	98.33	96.08	97.08
MagFace	ID-Overlap-C	99.82	98.41	92.92	98.23	96.17	97.11
AdaFace	ID-Disjoint	99.78	98.47	93.22	98.01	96.07	97.11
AdaFace	ID-Overlap-R	99.78	98.51	93.15	98.08	96.05	97.11
AdaFace	ID-Overlap-C	99.83	98.54	93.25	98.12	96.12	97.17

Table 1: Optimistic Bias In Accuracy From Train / Test Identity Overlap. ID-Disjoint = trained with a subset of MS1MV2 that has no overlap of identities with the particular test set. ID-Overlap-R (raw) = trained with a subset of MS1MV2 the same size as ID-Disjoint but without removing the identity overlap. ID-Overlap-C (cleaned) = ID-Overlap-R but correcting the identity label noise found as a result of determining identity overlap. Average accuracy estimated with ID-Overlap-R is higher or the same as with ID-Disjoint, representing the optimistic bias in accuracy from train/test identity overlap. Average accuracy estimated with ID-Overlap-C is higher still, showing that a cleaner training set increases the optimistic bias from train/test identity overlap. Columns in gray are the results on LFW and its variations.

	ArcFace	UniFace	MagFace	AdaFace
Original	97.14	97.13	97.08	97.17
ID-Overlap-C	97.16	97.12	97.11	97.17

Table 2: Average accuracy of four face recognition methods, trained with original and ID-Overlap-C MS1MV2, on five standard test sets.

model trained using the original MS1MV2 dataset. It is noteworthy that the ID-Overlap-C MS1MV2 version features 148K fewer images and 2,338 fewer identities than the original for LFW, 59K fewer images and 1,191 fewer identities for CFP-FP, and 87K fewer images and 2,091 fewer identities for AgeDB-30. **Hence, ensuring identity disjoint train and test sets is essential to eliminate the optimistic bias in performance measurement.**

4 Hadrian and Eclipse

Facial hairstyle and over / under-expose of the face region have been reported to significantly affect recognition accuracy across demographic groups [41, 44, 26, 40]. However, to date, there are no test sets that emphasize either of these two factors. Also, the previous section shows that the train and test sets should be identity-disjoint to avoid optimistic bias in the accuracy estimate. Therefore, we curated new test sets to focus on facial hairstyle (Hadrian) and under/over-exposure of the face region (Eclipse), as well as to eliminate identity overlap between the new test sets and popular in-the-wild training sets, and to enable comparison across demographic groups.

MORPH5 [30] was assembled from public records. Images were acquired under controlled conditions, including nominally frontal pose, neutral expression, consistent indoor lighting, and a uniform gray background. Age and demographic meta-data is associated with each image. The two demographics most represented in MORPH are African-American and Caucasian.

4.1 Selection of Facial Hairstyle Pairs for Hadrian

Facial hair attributes were predicted (using the model from [43]) for 155,683 images from 21,106 African-American males (AAM) and 97,666 images from 10,891 Caucasian males (CM). The facial hairstyle classification consists of detailed attributes, including beard area, beard length, and mustache.

Prior research [41, 44] has shown that a larger difference in facial hair attributes decreases similarity values, and that pairs with mustaches exhibit the highest similarity values. Therefore, to represent challenging facial hairstyle conditions, our target attributes were clean-shaven with no mustache (no-facial-hair) and those with a mustache connected to a full beard (full-facial-hair). Genuine pairs for the test set are targeted to be {no-facial-hair, full-facial-hair}, and impostor pairs are targeted to be {full-facial-hair, full-facial-hair}. To ensure accurate selection of images for facial hair attribute pairs, a threshold of 0.9 was applied for the algorithm in [43], resulting in 21,366 CM and 15,481 AAM images classified as no-facial-hair, and 21,831 CM and 23,221 AAM images classified as full-facial-hair. We used the aforementioned face matcher to extract features and calculate the similarity for both genuine and impostor pairs for AAM and CM independently. We randomly chose 7,000 genuine and impostor pairs, respectively, for further analysis. Allowing for the possibility of some identity label noise, impostor pairs with a similarity value higher than 0.7 and genuine pairs with similarity lower than 0.3 were excluded from selection.

MORPH5 has a range of age for each identity. To mitigate impact of age differences, we excluded genuine pairs with an age difference greater than 5 years. Additionally, to prevent any single image from disproportionately influencing the results, we restricted each image to occur in no more than 3 genuine and 3 impostor pairs. These measures reduced the number of genuine pairs to 2,205 for AAM and 1,635 for CM, and impostor pairs to 4,180 for AAM and 1,574 for CM.

We noted that the selected image pairs still exhibited identity label noise and inaccuracies in attribute pairs. Examples are in the Supplementary Material. Therefore, we performed a manual review to identify and rectify identity label noise, closely matched facial hairstyles in genuine pairs, and significantly different facial hair styles in impostor pairs. As a result, 543 genuine pairs and 279 impostor pairs were eliminated due to incorrect attribute pairing, and 44 pairs were discarded due to identity label noise.

Hadrian consists of 1,500 AAM genuine pairs, 1,500 AAM impostor pairs, 1,500 CM genuine pairs, and 1,500 CM impostor pairs. Similar to LFW [12], CFP-FP [33], CPLFW [45], CALFW [46], and AgeDB30 [25], accuracy is estimated as the mean accuracy from 10-fold cross-validation. In line with the format of previous test sets, each of the 10 folds contains 300 genuine and 300 impostor pairs. We arranged the image pairs by identity to ensure that the genuine pairs of each fold do not share identities with the genuine pairs in other folds, which is an aspect overlooked in earlier datasets.

4.2 Selection of Under- / Over-exposure Pairs for Eclipse

Wu et al. [40] categorized MORPH3 into five exposure groups: Strongly Underexposed (SU), Underexposed (U), Middle-exposed (M), Overexposed (O), and Strongly Overexposed (SO), based on percentile boundaries of face region brightness. To create a challenging face exposure test set, the ideal composition for genuine pairs would be (SU,SO), and for impostor pairs, (SO,SO) or (SU,SU). However, applying the same percentile boundaries used by [40] for image selection significantly reduces the capacity of the image pool, given that MORPH is a controlled-acquisition dataset.

To eliminate the influence of facial hair, only no-facial-hair images were included in Eclipse. Specifically, it comprises 15,481 African-American male (AAM) images, 20,630 African-American female (AAF) images, 21,366 Caucasian male (CM) images, and 157,025 Caucasian female (CF) images. Following the methodology of [40], we determined the exposure level for each face image and then selected images from the tails of the exposure distribution for each demographic group. The initial candidate pool was 25% of AAM images, 20% of AAF images, 20% of CM images, and 15% of CF images from both the upper tail for the high exposure image pool and the lower tail for the low exposure image pool. To identify the most challenging pairs, we used the same face matcher to extract the features and calculated the similarity of genuine and impostor pairs. Genuine pairs were defined as (high exposure, low exposure), and impostor pairs as either (high exposure, high exposure) or (low exposure, low exposure). Using the same threshold values of Hadrian to minimize identity label noise, we selected 2,098 AAF, 1,808 AAM, 7,000 CF, and 3,870 CM pairs for genuine pairs, and 6,000 impostor pairs for each demographic group in both scenarios. After controlling for age differences and image occurrence frequency, the most difficult 1,000 image pairs were chosen for both genuine and impostor pairs across each demographic. To curate the dataset further, a manual review was conducted to drop identity noise and drop misclassified exposure attribute pairs. Examples are in the

	# of IMs	# of IDs	Focus	Max _{occur}	Train _{Disj}	Demog _B
LFW [12]	7,701	4,281	General	12	✗	✗
CPLFW [45]	5,984	2,296	Pose	13	✗	✗
TALFW [47]	7,701	4,281	Attack	12	✗	✗
CALFW [46]	7,156	2,996	Age	11	✗	✗
MLFW [37]	7,156	2,996	Mask	11	✗	✗
XQLFW [20]	7,263	3,743	Image Quality	8	✗	✗
CFP-FP [33]	4,366	500	Pose	24	✗	✗
AgeDB-30 [25]	5,298	388	Age	28	✗	✗
DoppelVer [36]	27,693	390	Doppelgänger	82	✗	✗
Hadrian	7,646	2,600	Facial Hair	6	✓	✓
Eclipse	8,254	4,182	Face Exposure	6	✓	✓

Table 3: Statistical information of existing and proposed 10-Fold cross-validation test sets. Maximum occurrence of an image (Max_{occur}), identity disjoint to the training sets (Train_{Disj}), and equal number of images across demographics (Demog_B) are involved to reflect the feature of proposed dataset.

Supplementary Material. Ultimately, 225 genuine pairs, 184 (high exposure, high exposure) impostor pairs, and 379 (low exposure, low exposure) impostor pairs were excluded from the dataset.

Eclipse comprises 6,000 image pairs, with each demographic group contributing 750 genuine pairs and 750 impostor pairs. For each demographic, some impostor pairs have over-exposure in both images and some have under-exposure in both images. The rest of the dataset creation is the same as Hadrian.

4.3 Position in the “Zoo” of Test Sets

Various test sets have been developed to assess the accuracy of face recognition models. The two primary evaluation protocols are the 10-Fold cross-validation exemplified by LFW [12], and the True Accept Rate at False Accept Rate (TAR@FAR) exemplified by the IJB family [19, 38, 23]. The datasets proposed in this work align with the LFW paradigm, and so comparisons with the IJB family are not included.

Table 3 illustrates the rapid expansion of the LFW test set family to cover diverse challenges such as pose [45], age [46], occlusion [37], adversarial attacks [47], and image quality [20]. In addition to these, AgeDB-30 [25] and CFP-FP [33] are widely recognized for age difference. A recent dataset, DoppelVer [36], is for model evaluation on doppelgänger [36] pairs. In contrast with these test sets, the distinct advantages of the Hadrian and Eclipse test sets include:

Identity-Disjoint to Training Sets : Section 3 reveals that test sets such as LFW, CFP-FP, and AgeDB-30 share some identities with MS1MV2, Glint360K, and WebFace4M, which leads to optimistic estimates of face recognition accuracy. This issue, potentially applicable to other LFW variants, is inherently avoided in our new test sets. In addition, our test sets ensure identity disjoint genuine pairs across the 10 folds, which significantly impacts the accuracy measurement, as shown in Section 5.2. To our knowledge, this detail is overlooked in previous test sets.

Lower Repetition of Images Across Pairs : The difficulty level of a test set is often influenced by the frequency of challenging examples or noise, which themselves result from a variety of difficult factors. To maintain integrity and focus of the proposed datasets, we limited the occurrence of each image to no more than 6 times (i.e., no more than 3 times for both genuine and impostor pairs).

Balance Across Demographics : Employing the FairFace [17] classifier, we evaluated the gender and race distribution in LFW, CFP-FP, and AgeDB-30, as shown in Figure 3. The dominance of “White” individuals in these datasets implies that models performing best on these datasets may not achieve similar success across other racial groups. Our proposed datasets ensure an equal number of image pairs for each demographic group, providing a more comprehensive estimate of model accuracy.



Methods	Venue	LFW	CFP-FP	CPLFW	AgeDB-30	CALFW	Hadrian	Eclipse
ArcFace[6]	CVPR19	99.80	98.49	93.35	98.00	96.05	91.45	81.27
CurricularFace [13]	CVPR20	99.78	98.44	92.95	98.05	96.08	91.13	81.58
MagFace[24]	CVPR21	99.82	98.40	92.95	98.22	96.02	92.65	82.37
AdaFace[18]	CVPR22	99.82	98.63	93.05	98.20	96.15	92.05	82.03
UniFace[48]	ICCV23	99.78	98.49	93.28	98.02	96.10	91.38	82.08
ArcFace	CVPR19	99.77	99.21	94.27	97.85	96.12	91.62	83.20
CurricularFace	CVPR20	99.82	99.04	94.30	97.93	95.98	90.20	81.73
MagFace	CVPR21	99.80	99.23	94.18	97.88	95.97	90.80	82.27
AdaFace	CVPR22	99.78	99.14	94.32	97.63	96.13	90.50	82.28
UniFace	ICCV23	99.77	99.21	94.47	97.60	96.02	90.47	81.52
ArcFace	CVPR19	99.82	99.07	94.68	98.30	96.15	95.65	83.95
CurricularFace	CVPR20	99.78	99.11	94.68	98.43	96.17	94.05	83.38
MagFace	CVPR21	99.82	99.14	94.47	98.20	96.15	94.97	83.60
AdaFace	CVPR22	99.78	99.22	95.05	98.35	96.07	95.27	83.23
UniFace	ICCV23	99.73	99.09	94.58	98.22	96.18	93.53	82.53

Table 4: Performance of face recognition methods trained with ResNet100 backbone on previous benchmark datasets and ours. Methods are trained on MS1MV2 (Top), WebFace4M(Middle), and Glint360K(Bottom). [Keys: **Lowest two**]

	ArcFace	CurricularFace	MagFace	AdaFace	UniFace
MS1MV2	99.82	99.83	99.83	99.78	99.82
WebFace4M	99.83	99.80	99.82	99.83	99.82
Glint360K	99.83	99.85	99.83	99.82	99.82

Table 5: Ablation Study for Domain Effect. Accuracy for a test set randomly selected from MORPH5 is extremely high. Thus the challenging nature Hadrian and Eclipse does not come from the image domain, but from the designed emphasis on facial hairstyles and under-/over-exposure.

More Challenging : Table 4 presents the accuracy values of five face recognition methods, each trained using the original MS1MV2, WebFace4M, and Glint360K datasets, across five standard test sets and Hadrian and Eclipse. It is important to note that all models underwent training on the same platform, as detailed in Section 3, ensuring consistency in both training and testing procedures, albeit with the default configurations for each method. The results reveal that the average accuracy on CPLFW, the most challenging dataset prior to this study, is 1.7% higher than on Hadrian, and 11.57% higher than on Eclipse. Given that the MORPH images are recognized as good quality and controlled backgrounds, this underscores the greater challenge posed by the Hadrian and Eclipse test sets, emphasizing specific factors not recognized in previous test sets.

5 Ablation Study

MORPH5 [30] images can be considered as from a different source domain, controlled image acquisition, compared to the training and test sets that contain web-scraped, in-the-wild images. Also, none of the existing test sets enforce identity-disjoint folds in the 10-fold cross-validation. This section reports ablation results exploring the importance of these factors.

5.1 Hadrian and Eclipse Difficulty Not Due to Domain Shift

The current popular train and test sets all contain web-scraped, in-the-wild images, whereas the Eclipse and Hadrian images are from a controlled acquisition scenario. Previous research [34, 16] suggests that a change in the data domain can impact face recognition accuracy. Therefore, we conducted an ablation experiment to consider whether the challenging nature of Hadrian and Eclipse could be due simply to domain, rather than the intentional design emphasizing facial hairstyles and under-/over-exposure.

	ArcFace	CurricularFace	MagFace	AdaFace	UniFace
Hadrian-Disjoint	91.45	91.13	92.65	92.05	91.38
Hadrian-Overlap	91.72	91.42	92.68	92.35	91.48
Δ Hadrian	-0.27	-0.29	-0.03	-0.30	-0.10
Eclipse-Disjoint	81.27	81.58	82.37	82.03	82.08
Eclipse-Overlap	81.68	81.92	82.48	82.22	82.18
Δ Eclipse	-0.41	-0.34	-0.11	-0.19	-0.10

Table 6: Ablation study for identity overlap between folds. Δ is calculated by (Disjoint - Overlap). The methods are trained with ResNet100 on MS1MV2 dataset.

We curated another dataset from MORPH with the same number of identities and images, 750 genuine and 750 impostor pairs from each of Caucasian male, Caucasian female, African-American male and African-American female, totaling 6,000 pairs. Identities were randomly chosen for each demographic, without regard to facial hairstyle or under-/over-exposure. The final test set follows the LFW structure, where each of the 10 folds contains 300 genuine pairs and 300 impostor pairs, with the four demographic groups evenly distributed among the 300 image pairs. Comparing Table 5 and Table 4 reveals that the randomly-selected MORPH5 test set is the easiest dataset (has highest accuracy) for the five different matchers. Thus, the image source domain does not contribute to the challenging nature of Hadrian and Eclipse. In fact, the MORPH5 image domain is easier than the existing in-the-wild test sets, as might be expected.

5.2 Identity Disjoint Between Folds Is Necessary

For the 10-fold cross-evaluation, each time, 9 folds are regarded as the training set to find the best threshold distance to apply on 10-th fold (test set) in order to calculate the accuracy. This naturally brings up the question - *Does identity overlap across the folds affect the accuracy estimate?* To answer this, we used the same pairs in Hadrian and Eclipse but assigned genuine pairs of the same identity to different folds and kept everything else the same. In this case, identities in the test fold have the possibility to occur in the 9 train folds. Table 6 shows that having the test identities in the train sets significantly increases the accuracy value across five SOTA methods. Note that the difference between the average accuracy of the re-trained methods on MS1MV2 is 0.11%, but the average accuracy decrease is 0.2% on Hadrian and 0.23% on Eclipse across five methods. This means that identity-disjoint folds are necessary for constructing a 10-fold cross-evaluation test set.

6 Conclusions and Discussion

The widely used web-scraped test sets LFW, CPLFW, CALFW, CFP-FP and AgeDB-30 have identity overlap and even image overlap with web-scraped training sets such as MS1MV2, Glint360k and WebFace4M. To explore the effect of train/test identity overlap on the estimated accuracy, we curated three equal-size subsets of MS1MV2 – ID-Disjoint, ID-Overlap-R, and ID-Overlap-C – relative to each of the test sets LFW, CFP-FP and AgeDB-30. Results across four different face recognition methods demonstrate that accuracy estimation is given an optimistic bias when there is train / test identity overlap, and that this bias is larger with the training set is cleaner and the test set is more challenging. These results motivate a general recommendation in favor of identity-disjoint train and test sets, and also identity-disjoint folds in the test set, in order to obtain rigorous and unbiased accuracy estimates.

We curated two new face verification test sets following the general structure of existing test sets, but focused on dimensions of difficulty that are not emphasized in any existing test set. The Hadrian test set focuses on challenging facial hairstyle pairings and the Eclipse test set focuses on challenging under- / over-exposures pairings. To maintain the focus of each dataset, the effects of facial hairstyle are minimized in Eclipse and the effects of under- / over-exposure are minimized in Hadrian. Curating these test sets from the MORPH dataset ensures that they are identity-disjoint with all popular web-scraped training sets. Hadrian and Eclipse are new challenging test sets, with all models evaluated achieving lower accuracy than on the commonly-used existing LFW, CPLFW, CALFW, CFP-FP and AgeDB-30. An experimental comparison using a test set randomly selected from MORPH without regard to facial hairstyle and under-/over-exposure demonstrates that it is in fact the facial hairstyle combinations and exposure combinations that cause the challenging nature of these test sets.

References

- [1] Vítor Albiero and Kevin W Bowyer. Is face recognition sexist? no, gendered hairstyles and biology are. *BMVC*, 2020.
- [2] Xiang An, Xuhan Zhu, Yuan Gao, Yang Xiao, Yongle Zhao, Ziyong Feng, Lan Wu, Bin Qin, Ming Zhang, Debing Zhang, and Ying Fu. Partial FC: training 10 million identities on a single machine. In *ICCVW*, pages 1445–1449, 2021. URL <https://doi.org/10.1109/ICCVW54120.2021.00166>.
- [3] Aman Bhatta, Vítor Albiero, Kevin W Bowyer, and Michael C King. The gender gap in face recognition accuracy is a hairy problem. In *WACVW*, pages 303–312, 2023.
- [4] Jie Chen, Dong Yi, Jimei Yang, Guoying Zhao, Stan Z Li, and Matti Pietikainen. Learning mappings for face synthesis from near infrared to visual light images. In *CVPR*, pages 156–163, 2009.
- [5] Zhiyi Cheng, Xiatian Zhu, and Shaogang Gong. Low-resolution face recognition. In *ACCV*, pages 605–621, 2019.
- [6] Jiankang Deng, Jia Guo, Niannan Xue, and Stefanos Zafeiriou. Arcface: Additive angular margin loss for deep face recognition. In *CVPR*, pages 4690–4699, 2019. URL http://openaccess.thecvf.com/content_CVPR_2019/html/Deng_ArcFace_Additive_Angular_Margin_Loss_for_Deep_Face_Recognition_CVPR_2019_paper.html.
- [7] Jiankang Deng, Jia Guo, Debing Zhang, Yafeng Deng, Xiangju Lu, and Song Shi. Lightweight face recognition challenge. In *ICCVW*, pages 2638–2646. IEEE, 2019. URL <https://doi.org/10.1109/ICCVW.2019.00322>.
- [8] Mislav Grgic, Kresimir Delac, and Sonja Grgic. Sface—surveillance cameras face database. *Multimedia tools and applications*, 51:863–879, 2011.
- [9] Jianzhu Guo, Xiangyu Zhu, Zhen Lei, and Stan Z Li. Face synthesis for eyeglass-robust face recognition. In *CCBR*, pages 275–284, 2018.
- [10] Kaiming He, Xiangyu Zhang, Shaoqing Ren, and Jian Sun. Deep residual learning for image recognition. In *CVPR*, pages 770–778, 2016.
- [11] D Huang, J Sun, and Y Wang. The buaa-visnir face database instructions. *School Comput. Sci. Eng., Beihang Univ., Beijing, China, Tech. Rep. IRIP-TR-12-FR-001*, 3(3):8, 2012.
- [12] Gary B Huang, Marwan Mattar, Tamara Berg, and Eric Learned-Miller. Labeled faces in the wild: A database for studying face recognition in unconstrained environments. In *Workshop on faces in 'Real-Life' Images: detection, alignment, and recognition*, 2008.
- [13] Yuge Huang, Yuhan Wang, Ying Tai, Xiaoming Liu, Pengcheng Shen, Shaoxin Li, Jilin Li, and Feiyue Huang. Curricularface: Adaptive curriculum learning loss for deep face recognition. In *CVPR*, pages 5900–5909, 2020. URL https://openaccess.thecvf.com/content_CVPR_2020/html/Huang_CurricularFace_Adaptive_Curriculum_Learning_Loss_for_Deep_Face_Recognition_CVPR_2020_paper.html.
- [14] Isabelle Hupont and Carles Fernández Tena. Demogpairs: Quantifying the impact of demographic imbalance in deep face recognition. In *IEEE F&G*, pages 1–7, 2019. URL <https://doi.org/10.1109/FG.2019.8756625>.
- [15] Nathan D Kalka, Brianna Maze, James A Duncan, Kevin O’Connor, Stephen Elliott, Kaleb Hebert, Julia Bryan, and Anil K Jain. Ijb-s: Iarpa janus surveillance video benchmark. In *IEEE BTAS*, pages 1–9, 2018.
- [16] Meina Kan, Junting Wu, Shiguang Shan, and Xilin Chen. Domain adaptation for face recognition: Targetize source domain bridged by common subspace. *IJCV*, 109:94–109, 2014.
- [17] Kimmo Karkkainen and Jungseock Joo. Fairface: Face attribute dataset for balanced race, gender, and age for bias measurement and mitigation. In *WACV*, pages 1548–1558, 2021.

- [18] Minchul Kim, Anil K. Jain, and Xiaoming Liu. Adaface: Quality adaptive margin for face recognition. In *CVPR*, pages 18729–18738, 2022. URL <https://doi.org/10.1109/CVPR52688.2022.01819>.
- [19] Brendan F. Klare, Ben Klein, Emma Taborsky, Austin Blanton, Jordan Cheney, Kristen Allen, Patrick Grother, Alan Mah, Mark James Burge, and Anil K. Jain. Pushing the frontiers of unconstrained face detection and recognition: IARPA janus benchmark A. In *CVPR*, 2015. URL <https://doi.org/10.1109/CVPR.2015.7298803>.
- [20] Martin Knoche, Stefan Hormann, and Gerhard Rigoll. Cross-quality lfw: A database for analyzing cross-resolution image face recognition in unconstrained environments. In *IEEE F&G*, pages 1–5, 2021.
- [21] Stan Li, Dong Yi, Zhen Lei, and Shengcai Liao. The casia nir-vis 2.0 face database. In *CVPRW*, pages 348–353, 2013.
- [22] Ziwei Liu, Ping Luo, Xiaogang Wang, and Xiaoou Tang. Deep learning face attributes in the wild. In *ICCV*, pages 3730–3738, 2015.
- [23] Brianna Maze, Jocelyn C. Adams, James A. Duncan, Nathan D. Kalka, Tim Miller, Charles Otto, Anil K. Jain, W. Tyler Niggel, Janet Anderson, Jordan Cheney, and Patrick Grother. IARPA janus benchmark - C: face dataset and protocol. In *International Conference on Biometrics*, pages 158–165, 2018. URL <https://doi.org/10.1109/ICB2018.2018.00033>.
- [24] Qiang Meng, Shichao Zhao, Zhida Huang, and Feng Zhou. Magface: A universal representation for face recognition and quality assessment. In *CVPR*, pages 14225–14234, 2021. URL https://openaccess.thecvf.com/content/CVPR2021/html/Meng_MagFace_A_Universal_Representation_for_Face_Recognition_and_Quality_Assessment_CVPR_2021_paper.html.
- [25] Stylianos Moschoglou, Athanasios Papaioannou, Christos Sagonas, Jiankang Deng, Irene Kotsia, and Stefanos Zafeiriou. Agedb: The first manually collected, in-the-wild age database. In *CVPRW*, pages 1997–2005, 2017. URL <https://doi.org/10.1109/CVPRW.2017.250>.
- [26] Kagan Ozturk, Grace Bezold, Aman Bhatta, Haiyu Wu, and Kevin Bowyer. Beard segmentation and recognition bias. *arXiv preprint arXiv:2308.15740*, 2023.
- [27] P Jonathon Phillips, Patrick J Flynn, Kevin W Bowyer, Richard W Vorder Bruegge, Patrick J Grother, George W Quinn, and Matthew Pruitt. Distinguishing identical twins by face recognition. In *IEEE F&G*, pages 185–192, 2011.
- [28] Anant Ram, Sunita Jalal, Anand S Jalal, and Manoj Kumar. A density based algorithm for discovering density varied clusters in large spatial databases. *International Journal of Computer Applications*, 3(6):1–4, 2010.
- [29] Christian Rathgeb, Pawel Drozdowski, Marcel Obel, André Dörsch, Fabian Stockhardt, Nathania E Haryanto, Kevin Bernardo, and Christoph Busch. Impact of doppelgänger on face recognition: Database and evaluation. In *IEEE BIOSIG*, pages 1–4, 2021.
- [30] Karl Ricanek and Tamirat Tesafaye. Morph: A longitudinal image database of normal adult age-progression. In *IEEE F&G*, pages 341–345, 2006.
- [31] Joseph P. Robinson, Gennady Livitz, Yann Henon, Can Qin, Yun Fu, and Samson Timoner. Face recognition: Too bias, or not too bias? In *CVPRW*, pages 1–10, 2020. URL https://openaccess.thecvf.com/content_CVPRW_2020/html/w1/Robinson_Face_Recognition_Too_Bias_or_Not_Too_Bias_CVPRW_2020_paper.html.
- [32] Torsten Schlett, Christian Rathgeb, Juan Tapia, and Christoph Busch. Double trouble? impact and detection of duplicates in face image datasets. *arXiv preprint arXiv:2401.14088*, 2024.
- [33] Soumyadip Sengupta, Jun-Cheng Chen, Carlos Domingo Castillo, Vishal M. Patel, Rama Chellappa, and David W. Jacobs. Frontal to profile face verification in the wild. In *WACV*, pages 1–9, 2016. URL <https://doi.org/10.1109/WACV.2016.7477558>.

- [34] Kihyuk Sohn, Sifei Liu, Guangyu Zhong, Xiang Yu, Ming-Hsuan Yang, and Manmohan Chandraker. Unsupervised domain adaptation for face recognition in unlabeled videos. In *ICCV*, pages 3210–3218, 2017.
- [35] Philipp Terhörst, Jan Niklas Kolf, Marco Huber, Florian Kirchbuchner, Naser Damer, Aythami Morales Moreno, Julian Fierrez, and Arjan Kuijper. A comprehensive study on face recognition biases beyond demographics. *IEEE Transactions on Technology and Society*, 3(1):16–30, 2021.
- [36] Nathan Thom, Andrew DeBolt, Lyssie Brown, and Emily M Hand. Doppelver: A benchmark for face verification. In *International Symposium on Visual Computing*, pages 431–444. Springer, 2023.
- [37] Chengrui Wang, Han Fang, Yaoyao Zhong, and Weihong Deng. Mlfw: A database for face recognition on masked faces. *arXiv preprint arXiv:2109.05804*, 2021.
- [38] Cameron Whitelam, Emma Taborsky, Austin Blanton, Brianna Maze, Jocelyn C. Adams, Tim Miller, Nathan D. Kalka, Anil K. Jain, James A. Duncan, Kristen Allen, Jordan Cheney, and Patrick Grother. IARPA janus benchmark-b face dataset. In *CVPRW*, pages 592–600, 2017. URL <https://doi.org/10.1109/CVPRW.2017.87>.
- [39] Haiyu Wu and Kevin W Bowyer. What should be balanced in a” balanced” face recognition dataset. In *BMVC*, volume 1, page 2, 2023.
- [40] Haiyu Wu, Vitor Albiero, KS Krishnapriya, Michael C King, and Kevin W Bowyer. Face recognition accuracy across demographics: Shining a light into the problem. In *CVPRW*, pages 1041–1050, 2023.
- [41] Haiyu Wu, Grace Bezold, Aman Bhatta, and Kevin W Bowyer. Logical consistency and greater descriptive power for facial hair attribute learning. In *CVPR*, pages 8588–8597, 2023.
- [42] Haiyu Wu, Grace Bezold, Manuel Günther, Terrance Boulton, Michael C. King, and Kevin W. Bowyer. Consistency and accuracy of celeba attribute values. In *CVPRW*, 2023.
- [43] Haiyu Wu, Sicong Tian, Huayu Li, and Kevin W Bowyer. Logicnet: A logical consistency embedded face attribute learning network. *arXiv preprint arXiv:2311.11208*, 2023.
- [44] Haiyu Wu, Sicong Tian, Aman Bhatta, Kağan Öztürk, Karl Ricanek, and Kevin W Bowyer. Facial hair area in face recognition across demographics: Small size, big effect. In *WACVW*, pages 1131–1140, 2024.
- [45] Tianyue Zheng and Weihong Deng. Cross-pose lfw: A database for studying cross-pose face recognition in unconstrained environments. *Beijing University of Posts and Telecommunications, Tech. Rep*, 5(7), 2018.
- [46] Tianyue Zheng, Weihong Deng, and Jiani Hu. Cross-age lfw: A database for studying cross-age face recognition in unconstrained environments. *arXiv preprint arXiv:1708.08197*, 2017.
- [47] Yaoyao Zhong and Weihong Deng. Towards transferable adversarial attack against deep face recognition. *IEEE Transactions on Information Forensics and Security*, 2020.
- [48] Jiancan Zhou, Xi Jia, Qiufu Li, Linlin Shen, and Jinming Duan. Uniface: Unified cross-entropy loss for deep face recognition. In *ICCV*, pages 20730–20739, 2023.
- [49] Zheng Zhu, Guan Huang, Jiankang Deng, Yun Ye, Junjie Huang, Xinze Chen, Jiagang Zhu, Tian Yang, Dalong Du, Jiwen Lu, and Jie Zhou. Webface260m: A benchmark for million-scale deep face recognition. *PAMI*, 45(2):2627–2644, 2023. URL <https://doi.org/10.1109/TPAMI.2022.3169734>.

This supplementary material provides 1) Gender and race distribution of LFW, CALFW, and CPLFW - Figure 3, 2) detected mislabeling examples in MORPH5 - Figure 5 and Figure 4, 3) 20 image pairs of the detected identity overlap and image overlap between MS1MV2 and LFW, CFP-FP, AgeDB-30.

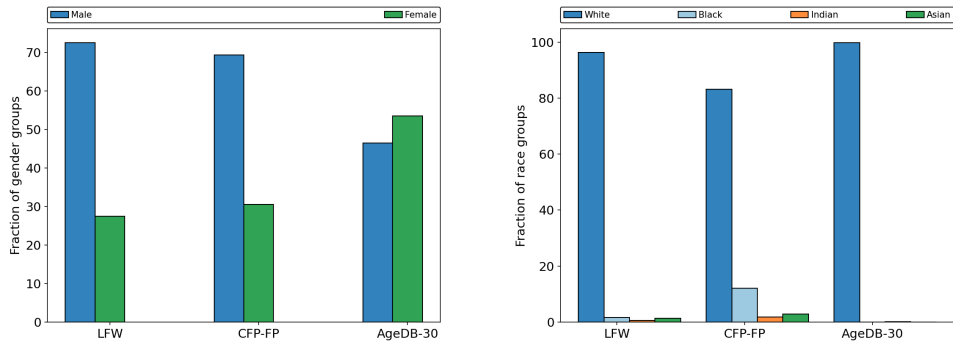


Figure 3: Gender (l) and Race (r) of Identities in LFW, CFP-FP and AgeDB-30.

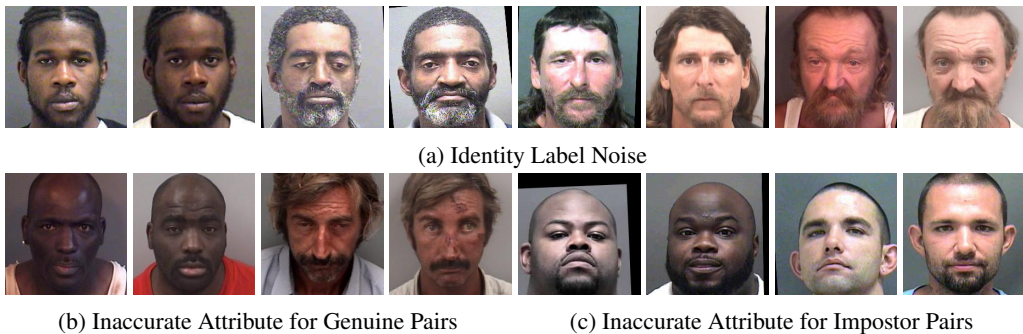


Figure 4: Examples of detected identity label noise (top) and inaccurate attribute pairs (bottom) when assembling **Hadrian**. For identity label noise, the images in each pair are labeled as different person but they are not. For inaccurate attribute pairs, images in each genuine pair should have large difference on facial hair attribute but they do not, and images in each impostor pair should have same full-facial-hair attribute but they are not.



(a) Opposite-exposure Genuine pairs



(b) High-exposure impostor pairs



(c) Low-exposure impostor pairs

Figure 5: Examples of detected inaccurate attribute pairs when assembling **Eclipse**. Since facial hair can affect the face recognition accuracy, a pair with a facial hair image are dropped.

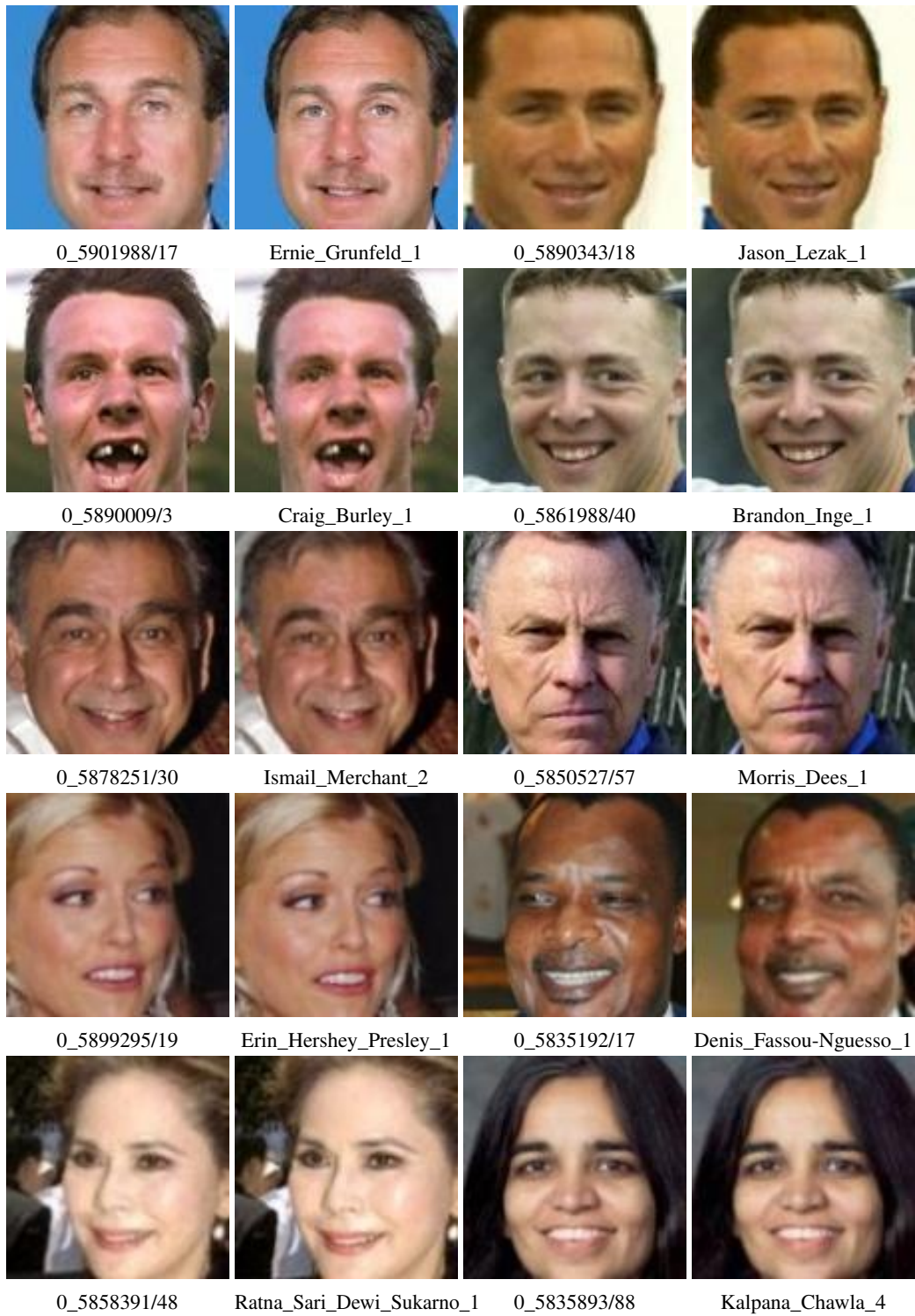


Figure 6: Examples of the same images occur in both LFW and MS1MV2.

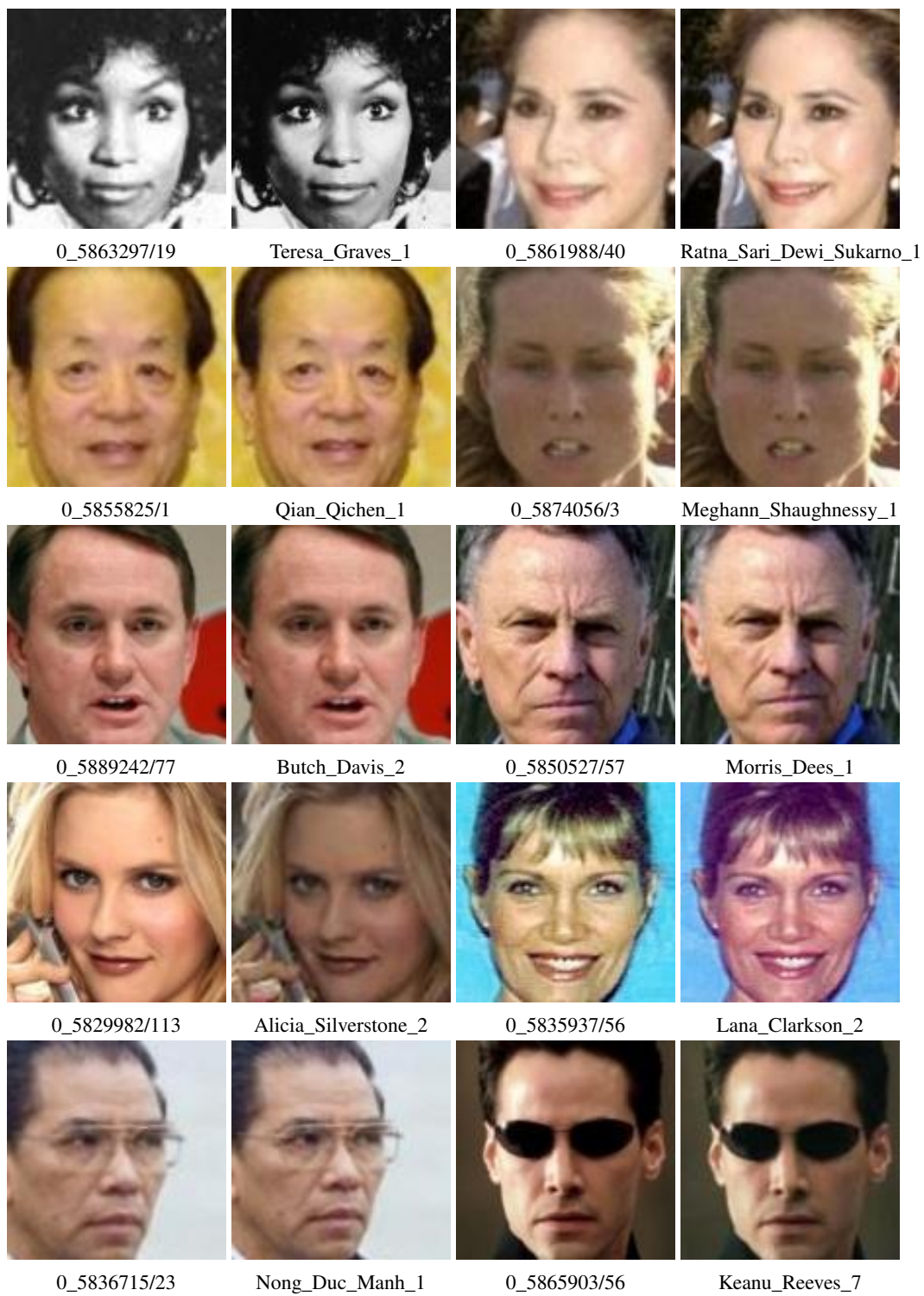


Figure 7: Examples of the same image occur in both LFW and MS1MV2.



Figure 8: Examples of the same images occur in both AgeDB-30 and MS1MV2.



Figure 9: Examples of the same image occur in both AgeDB-30 and MS1MV2.

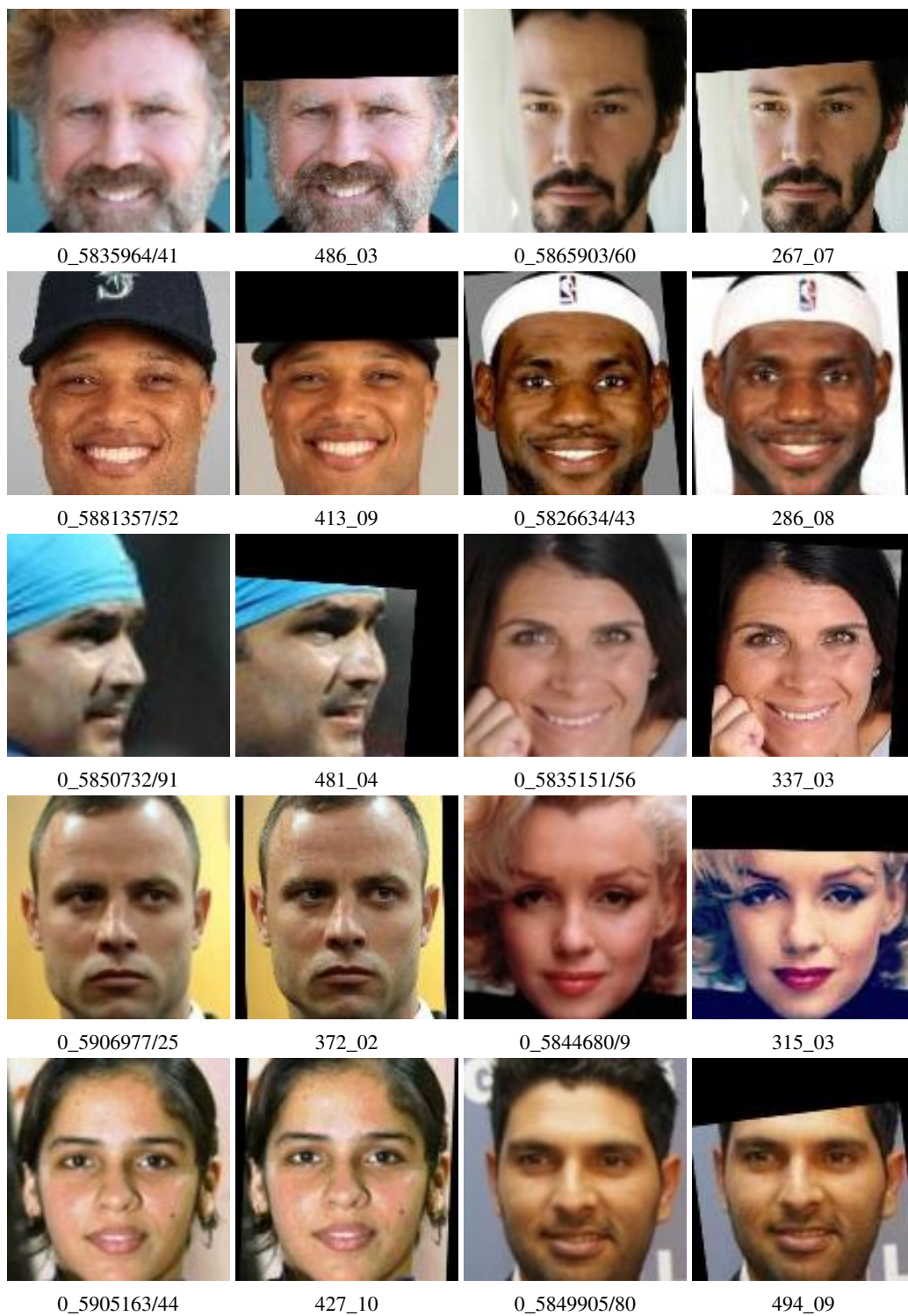


Figure 10: Examples of the same images occur in both CFP-FP and MS1MV2.



Figure 11: Examples of the same image occur in both CFP-FP and MS1MV2.



Figure 12: Examples of the same identity occur in both LFW and MS1MV2.



Figure 13: Examples of the same identity occur in both LFW and MS1MV2.

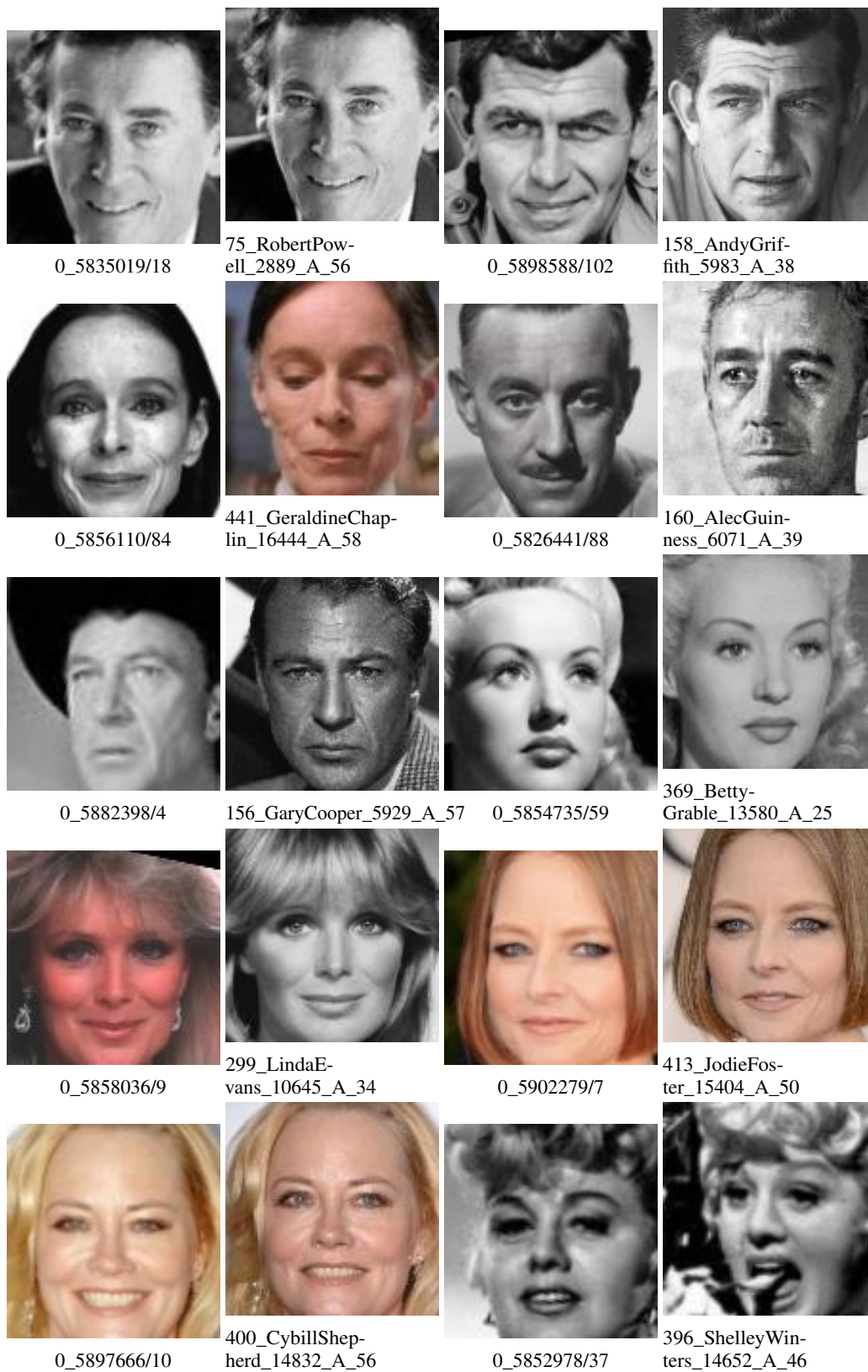


Figure 14: Examples of the same identity occur in both AgeDB-30 and MS1MV2.



Figure 15: Examples of the same identity occur in both AgeDB-30 and MS1MV2.

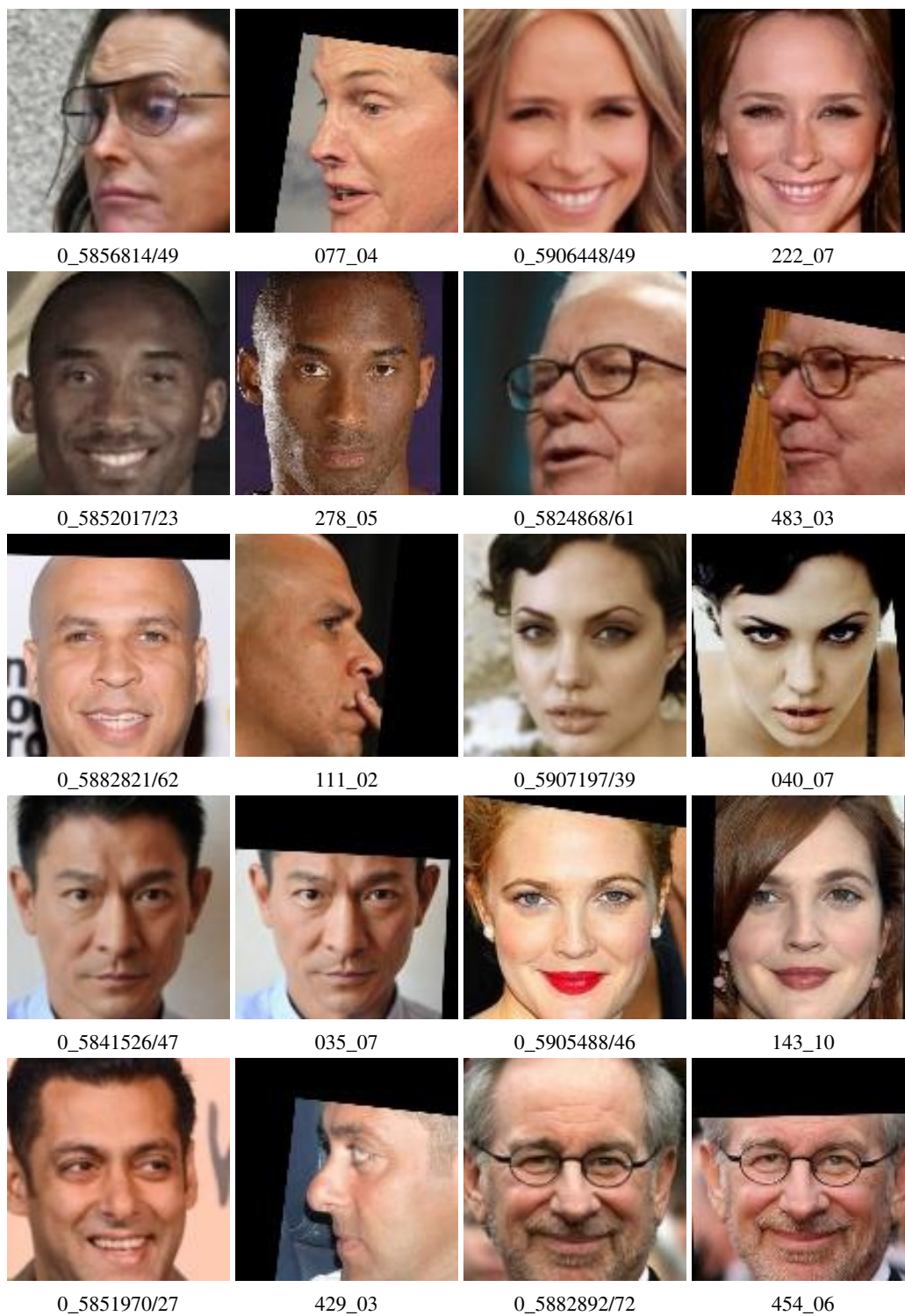


Figure 16: Examples of the same identity occur in both CFP-FP and MS1MV2.

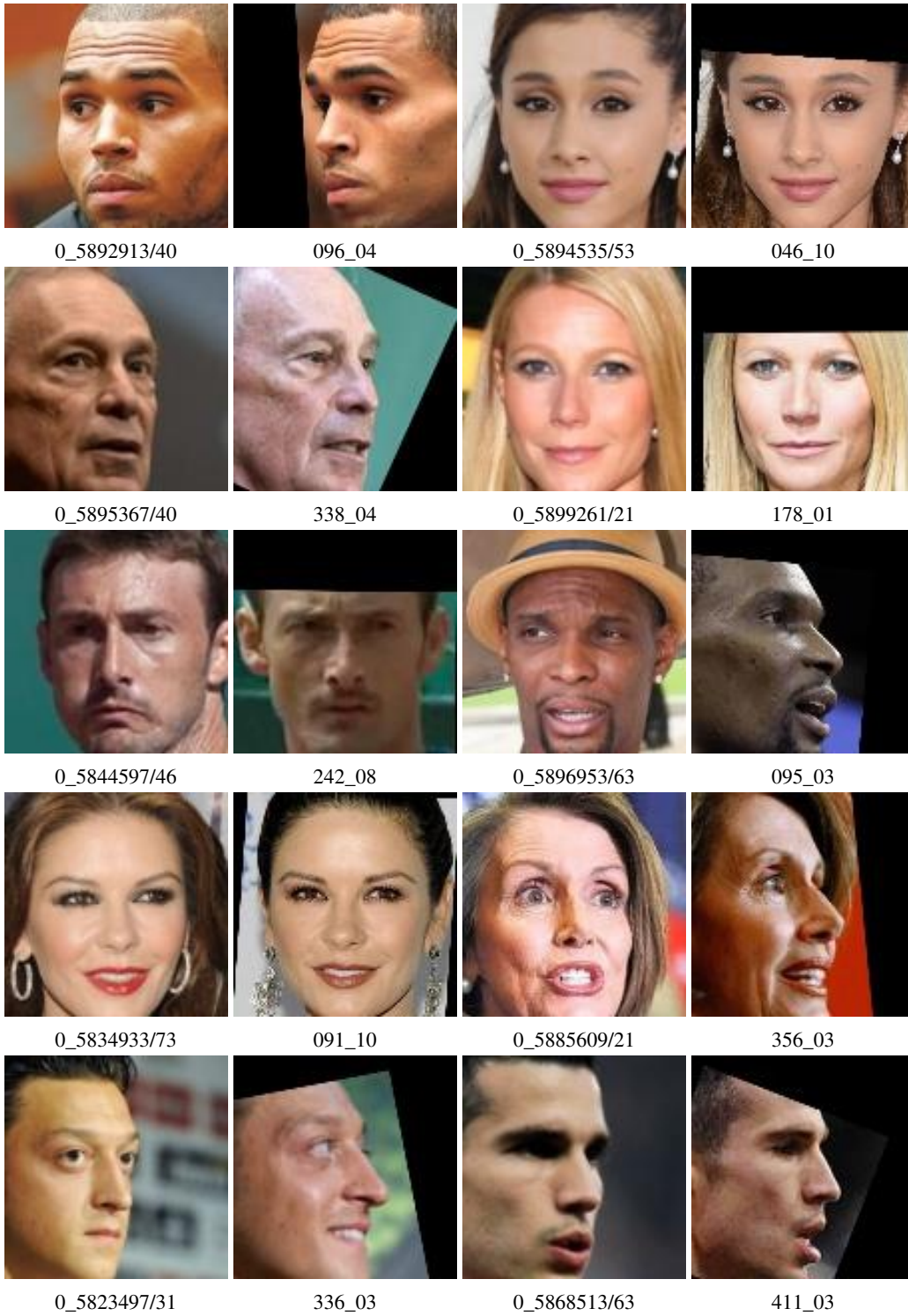


Figure 17: Examples of the same identity occur in both CFP-FP and MS1MV2.